

STUDY OF ELEMENTARY REACTIONS WITH
THE HADES DIELECTRON SPECTROMETER*

B. RAMSTEIN

Institut de Physique Nucléaire, CNRS/IN2P3-Université Paris Sud
91406 Orsay Cedex, France

G. AGAKICHIEV^h, C. AGODI^a, A. BALANDA^{c,e}, G. BELLIA^{a,w}, D. BELVER^o, A. BELYAEV^f
 A. BLANCO^b, M. BÖHMER^k, J.L. BOYARD^m, P. BRAUN-MUNZINGER^d, P. CABANELAS^o
 E. CASTRO^o, T. CHRIST^k, M. DESTEFANISⁿ, J. DÍAZ^p, F. DOHRMANN^e, A. DYBCZAK^c
 L. FABIETTI^k, O. FATEEV^f, P. FINOCCHIARO^a, P. FONTE^{b,s}, J. FRIESE^k, I. FRÖHLICH^g
 T. GALATYUK^d, J.A. GARZÓN^o, R. GERNHÄUSER^k, A. GIL^p, C. GILARDI^h, M. GOLUBEVA^j
 D. GONZÁLEZ-DÍAZ^d, E. GROSSE^{e,c}, F. GUBER^j, M. HELLMANN^g, T. HENNINO^m
 R. HOLZMANN^d, A. IERUSALIMOV^f, I. IORI^{i,u}, A. IVASHKIN^j, M. JURKOVIC^k, B. KÄMPFER^e
 K. KANAKI^e, T. KARAVICHEVA^j, D. KIRSCHNER^h, I. KOENIG^d, W. KOENIG^d, B.W. KOLB^d
 R. KOTTE^e, A. KOZUCH^{c,w}, A. KRÁSAⁿ, F. KRŮŽEKⁿ, R. KRÜCKEN^k, W. KÜHN^h
 A. KUGLERⁿ, A. KUREPIN^j, J. LAMAS-VALVERDE^o, S. LANG^d, J.S. LANGE^h, K. LAPIDUS^j
 L. LOPES^b, M. LORENZ^g, T. LIU^m, L. MAIER^k, A. MANGIAROTTI^b, J. MARÍN^o
 J. MARKERT^g, V. METAG^h, B. MICHALSKA^c, J. MICHEL^g, D. MISHRA^h, E. MORINIÈRE^m
 J. MOUSA^l, C. MÜNTZ^g, L. NAUMANN^e, R. NOVOTNY^h, J. OTWINOWSKI^c
 Y.C. PACHMAYER^g, M. PALKA^d, Y. PARPOTTAS^l, V. PECHENOV^h, O. PECHENOVA^h
 T. PÉREZ CAVALCANTI^h, J. PIETRASZKO^d, W. PRZYGODA^{c,w}, A. RESHETIN^j, A. RUSTAMOV^d
 A. SADOVSKY^j, P. SALABURA^c, A. SCHMA^{h,k}, R. SIMON^d, YU.G. SOBOLEVⁿ, S. SPATARO^h
 B. SPRUCK^h, H. STRÖBELE^g, J. STROTH^{g,d}, C. STURM^g, M. SUDOL^m, A. TARANTOLA^g
 K. TEILAB^g, P. TLUSTÝⁿ, M. TRAXLER^d, R. TREBACZ^c, H. TSSERTOS^l, I. VERETENKIN^j
 V. WAGNERⁿ, M. WEBER^k, M. WISNIOWSKI^c, J. WÜSTENFELD^e, S. YUREVICH^d
 Y.V. ZANEVSKY^f, P. ZHOU^d, P. ZUMBRUCH^e

^aIstituto Nazionale di Fisica Nucleare, Laboratori Nazionali del Sud, 95125 Catania, Italy^bLIP-Laboratório de Instrumentação e Física Experimental de Partículas, 3004-516 Coimbra, Portugal^cM. Smoluchowski Institute of Physics, Jagellonian University, 30-059 Kraków, Poland^dGSII Helmholtzzentrum für Schwerionenforschung, 64291 Darmstadt, Germany^eInstitut für Strahlenphysik, Forschungszentrum Dresden-Rossendorf, 01314 Dresden, Germany^fJoint Institute of Nuclear Research, 141980 Dubna, Russia^gInstitut für Kernphysik, Johann Wolfgang Goethe-Universität, 60438 Frankfurt, Germany^hII. Physikalisches Institut, Justus Liebig Universität Giessen, 35392 Giessen, GermanyⁱIstituto Nazionale di Fisica Nucleare, Sezione di Milano, 20133 Milano, Italy^jInstitute for Nuclear Research, Russian Academy of Science, 117312 Moscow, Russia^kPhysik Department E12, Technische Universität München, 85748 München, Germany^lDepartment of Physics, University of Cyprus, 1678 Nicosia, Cyprus^mInst. de Physique Nucléaire, CNRS/IN2P3-Université Paris Sud, 91406 Orsay Cedex, FranceⁿNuclear Physics Institute, Academy of Sciences of Czech Republic, 25068 Rez, Czech Republic^oDep. de Física de Partículas, Univ. de Santiago de Compostela, 15706 Santiago de Compostela, Spain^pInstituto de Física Corpuscular, Universidad de Valencia-CSIC, 46971 Valencia, Spain^qDipartimento di Fisica e Astronomia, Università di Catania, 95125 Catania, Italy^rISEC Coimbra, Coimbra, Portugal^tTechnische Universität Dresden, 01062 Dresden, Germany^uDipartimento di Fisica, Università di Milano, 20133 Milano, Italy^wState Higher Vocational School, 33-300 Nowy Sacz, Poland

(Received January 5, 2010)

* Presented at the XXXI Mazurian Lakes Conference on Physics, Piaski, Poland, August 30–September 6, 2009.

Results obtained with the HADES dielectron spectrometer at GSI are discussed, with emphasis on dilepton production in elementary reactions.

PACS numbers: 21.65.Jk, 25.75.-q, 25.75.Dw, 25.40.-h

1. Introduction

The main objective of the High-Acceptance di-Electron Spectrometer at GSI is the study of in-medium modifications of ρ and ω vector mesons in hot and/or dense baryonic matter. Despite the challenging instrumental requirements, the dilepton probe provides the most direct information on the hadronic matter. Being complementary to the ones performed at higher energy facilities (SPS, RHIC) or looking for effects at normal density with photon or proton beams (JLab, KEK), the HADES experiments explore the 1–2 AGeV energy domain, where moderate temperatures ($T < 100$ MeV) and baryonic densities up to 3 times the normal nuclear matter density can be achieved, with expected sizeable modifications of ρ and ω meson spectral functions. In contrast to reactions at ultrarelativistic energies, the multiplicity of produced pions per participant remains quite small, of the order of 10%. This presents major advantages, since the main source of combinatorial background is the conversion of photons from $\pi^0 \rightarrow \gamma\gamma$ or $\pi^0 \rightarrow \gamma e^+ e^-$.

Another specificity of the SIS-18 energy regime is the important role played by baryonic resonances. Due to the very long life-time (15 fm/c) of the dense hadronic matter phase, the resonance can propagate and regenerate and the modification of its spectral function inside the baryonic medium is therefore an important issue for transport model calculations.

The $\Delta(1232)$ resonance, which is responsible for a dominant part of the pion production, is the most copiously produced, but as the incident energy increases, higher lying resonances will play an increasing role. While all of them contribute to pion production, the $N(1535)$ for example is important for the η production and the $N(1520)$, $\Delta(1620)$ and others for the ρ production. Through the direct dilepton decay ($\rho/\omega \rightarrow e^+ e^-$) or Dalitz decay ($\pi^0/\eta \rightarrow \gamma e^+ e^-$ or $\omega \rightarrow \pi^0 e^+ e^-$) modes of these mesons, the baryonic resonances therefore play a crucial role in dilepton emission. They are also expected to contribute directly to dilepton emission via their own Dalitz decay modes. For example, the $\Delta(1232)$ should present a Dalitz decay (*e.g.* $\Delta \rightarrow N e^+ e^-$) branching ratio of 4.2×10^{-5} , according to QED calculations. As it has never been measured up to now, the experimental study of this decay mode is an experimental challenge. In addition, the Δ Dalitz decay process is in principle sensitive to the electromagnetic structure of the $N-\Delta$ transition and the kinematics is suited to test the Vector Dominance Models.

On the other hand, another important dilepton source in this energy range is the nucleon–nucleon Bremsstrahlung $NN \rightarrow NN e^+ e^-$, which adds coherently to the Δ Dalitz decay.

Sec. 2 will show how the first results of HADES in heavy-ion experiments motivate the study of elementary pp and pd reactions. In Sec. 3, the Δ Dalitz decay and NN virtual bremsstrahlung are discussed. Sec. 4 is devoted to the description of the experimental set-up and results from inclusive pp and quasi-free pn reactions. Exclusive measurements in pp collisions and perspectives of pion beam experiments are presented in Sec. 5 and 6, respectively.

2. First results from heavy-ion experiments

The first results from the HADES collaboration for the $^{12}\text{C}+^{12}\text{C}$ reaction at 1 and 2 AGeV [1, 2] have marked an important turning point. In these reactions, the dilepton production shows an excess in the intermediate mass range 0.15–0.6 GeV/ c^2 with respect to the long-lived source contribution, which is mainly due to the η Dalitz decay and is well constrained by experimental measurements. Such a dilepton excess had been already observed, more than 10 years ago, by the Dilepton Spectrometer (DLS) experiment at Berkeley [3] in the $^{12}\text{C}+^{12}\text{C}$ reaction at 1 AGeV and remained unexplained over years, the situation being known as the “DLS Puzzle”. Taking into account the much smaller DLS acceptance, a direct comparison of the two data sets was performed, showing very good agreement [2]. This confirmation of the DLS controversial results triggered new transport model calculations [4, 5] which are now able to reproduce the dilepton spectra measured in the $^{12}\text{C}+^{12}\text{C}$ reactions by DLS and HADES. In particular, the new HSD results are using the recent bremsstrahlung calculation from [6], which is a factor 2–4 higher than other calculations. According to the authors of [4], this provided the solution to the “DLS puzzle”. However, this bremsstrahlung prediction is contradicted by other approaches [7]. In addition, other transport model calculations reproduce quite well the excess with different relative contributions of bremsstrahlung and Δ Dalitz decay processes. More selective experimental constraints on these specific dilepton sources seem therefore necessary to achieve a satisfactory explanation of the intermediate mass dilepton production in the C+C system. This is even more important for heavier systems, like Ar+KCl, recently investigated by HADES [8] and where medium effects are looked for, since a reliable reference for “vacuum” dilepton production above η contribution is needed. This motivates the study of the $p+p$ and quasi-free $n+p$ reactions with HADES experiments at 1.25 GeV, *i.e.* below the η production threshold.

Another unavoidable requirement for interpretation of dilepton spectra in terms of medium effects, is a careful description of the vector meson production, which implies the knowledge of inclusive meson production cross-section. The first results [8] from the Ar+KCl reaction indeed show that this input might need to be readjusted in transport models. To measure it, the dilepton spectra in the $p + p$ reaction at 3.5 GeV have been analyzed. The results are still too preliminary, therefore, the focus will be in the following on the analysis of $p + p$ and $n + p$ reactions at 1.25 GeV. Results obtained in exclusive analysis at 2.2 GeV will also be presented in Sec. 6.

3. Δ Dalitz decay and NN Bremsstrahlung

3.1. Different theoretical approaches

The description of these processes has to combine the electromagnetic vertex, including the electromagnetic structure of the involved hadrons, parametrized by form factors and the nucleon–nucleon interaction. The Soft Photon Approximation (SPA) [9] offers a possible way to take both aspects into account, with a factorization of the photon emission probability and of the strong interaction process. It was found to be in reasonable agreement, at least for the pn case, where this process is the most important, with more complete calculations [7]. As a consequence, SPA is still widely used in transport model calculations, the Dalitz decay dilepton yield being calculated independently and added incoherently.

Although the differential decay width of the Δ Dalitz decay process derives in principle unambiguously from the QED vertex, different expressions can be found in the literature, as stressed in [10]. We checked ourselves these calculations and could confirm the expressions of [10] and [11]. Consistent spectra are provided by the other descriptions at the Δ resonance mass pole. However, taking as an example a mass of 1.480 GeV/ c^2 , corresponding to the kinematical limit for a pp reaction at 1.25 GeV, variations of the differential Dalitz decay width of 30% for M_{ee} close to zero to 65% at $M_{ee} = 0.5$ GeV/ c^2 are observed [12].

A reliable description of these processes can only be accessed in full quantum mechanical and gauge invariant calculations. Two One Boson Exchange (OBE) calculations [6, 13], which fulfill these requirements were performed recently and the yields were found a factor about 2–3 higher in [6] than in [13] for both pp and pn reactions, the second calculation being much closer to the SPA predictions. An experimental check of these predictions is therefore needed to clarify the situation.

As seen in Fig. 1 for an incident energy of 1.25 GeV, the Δ graphs are widely dominant in the case of the pp reaction, except above 400 MeV/ c^2 , while, for the pn reaction, the nucleon graphs are much more important.

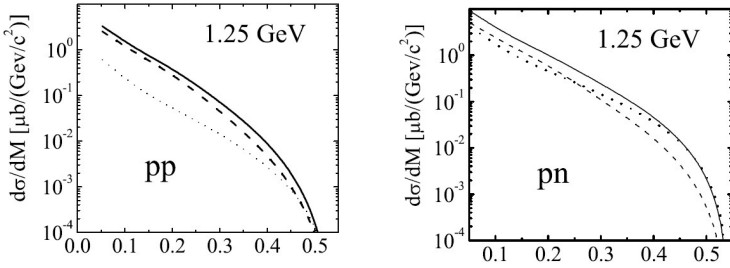


Fig. 1. Predictions for the dielectron mass distributions in the pp (left-hand side) and np (right-hand side) reactions at 1.25 GeV/nucleon [6]. Solid lines: full calculations; dashed lines: Δ graphs only; dotted lines: nucleon graphs only.

These qualitative features are common to both models, and show that, by measuring dilepton spectra in pp and np reactions, a selective sensitivity to these different graphs can be obtained.

3.2. Electromagnetic form-factors

Further important elements are the electromagnetic form factors, which are of two types, namely the elastic nucleon form factor and the N - Δ transition form factors. In both cases, the electromagnetic vertex is time-like, since the four-momentum transfer squared q^2 , which is equal to the squared dilepton mass, is a positive quantity. The influence of elastic nucleon form factors taken in Vector Dominance Models (VDM) has been studied in [6]. We will here discuss in more details the case of the N - Δ transition form factors. While, for negative four-momentum transfer squared (space-like region), the three N - Δ transition form factors (G_E , G_M and G_C as electric, magnetic and Coulomb form factors respectively) have been measured in pion- or photo-production experiments in a quite wide range of q^2 , the time-like region is unexplored. Here, the q^2 dependence can therefore only be given by models, constrained by the fact that the form factors have to be analytical functions of q^2 , and should reproduce the available space-like data. Due to the small q^2 values probed by the dilepton production in our reactions, the major requirement is that the values of the form factors at $q^2 = 0$ should be in agreement with the values from pion photoproduction experiments (photon point) and correlatively the radiative decay width ($\Gamma(\Delta \rightarrow \gamma N) = 0.66 \text{ MeV} \pm 0.06 \text{ MeV}$) should be well reproduced, as in [10, 11]. However, the kinematical region probed by the Δ Dalitz decay ($q^2 < 0.3(\text{GeV}/c)^2$ for an incident energy of 1.25 GeV) is of interest to check the Vector Dominance. In such a model, the electromagnetic baryon form factors present structures in the vicinity of the ρ meson mass, which might be probed by the Δ Dalitz decay process.

3.3. Analysis tool for $p + p$ and quasi-free $n + p$ reactions

The new developments of our event generator PLUTO [15, 16] were exploited in order to build efficient tools for the interpretation of our data. Two different approaches were followed:

The first one is based on the observation that, at an energy of 1.25 GeV per nucleon, pions are mostly produced through intermediate Δ resonances. In analogy with the description of the π^0 and Δ Dalitz decay in transport model calculations, it provides a description of the following channels:

$$\Delta^+ \rightarrow p\pi^0 \rightarrow p\gamma e^+e^-, \quad \Delta^+ \rightarrow pe^+e^-, \quad (1)$$

$$\Delta^0 \rightarrow n\pi^0 \rightarrow n\gamma e^+e^-, \quad \Delta^0 \rightarrow ne^+e^-. \quad (2)$$

The cross-sections of all the π^0 and related Δ^+ and Δ^0 channels are taken from the resonance model [17], which describes the existing data [17, 18], including as we will see in Sec. 4, the new measurements by HADES in the hadronic channels $pp \rightarrow pp\pi^0$. The details of the Δ production and decay are given in [15, 16]. For the Δ Dalitz decay differential width ($d\Gamma/dM$), the expression from [10] was adopted, as explained above and two options for the N - Δ transition form factors are provided: either a constant magnetic form factor ($G_M = 3$, in agreement with the photon-point measurements), or the two-component quark-model (Fig. 2) [14], which is mainly driven by the Vector Dominance in our energy range.

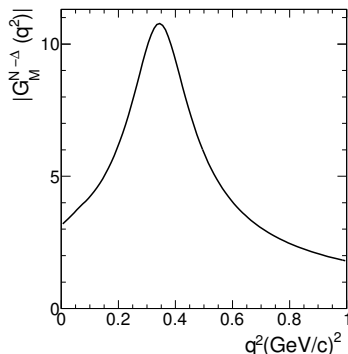


Fig. 2. Magnetic N - Δ transition form-factor squared from the two component quark model [14].

The second approach aims at a direct comparison with the OBE predictions. Hence, the differential cross-sections ($d\sigma/dM$) provided by the models [6, 13] have been parameterized, an isotropic virtual photon emission was further assumed and corrections due to Final State Interaction of the two outgoing nucleons were included.

To simulate the quasi-free $n + p$ reaction, the available energy in the center of mass was smeared to include the neutron momentum distribution in the deuteron using the Paris potential and the energy dependence of the cross-sections was taken into account. When the center of mass energy of the pn system exceeds the η threshold, its production is also taken into account, with cross-sections taken from existing data [19].

The generated events are then filtered by the detector acceptance in order to compare to the experimental data.

3.4. Experimental set-up

The HADES (High Acceptance Dielectron Spectrometer) detector (Fig. 3) consists in 6 identical sectors covering the full azimuthal range and polar angles between 18° and 85° , hence providing a lepton pair acceptance of the order of 0.35. A detailed description can be found in [20], thus only the main features are given here. Momentum measurement derives from the particle trajectory reconstruction using four Mini-Drift Chambers (two before and two after the magnetic field zone) providing a position resolution of about $140 \mu\text{m}$ per cell and a measured dilepton invariant mass resolution of about 2.4% at the ω meson mass. A hadron-blind Ring Imaging CHerenkov detector (RICH), made by a C_4F_{10} gas radiator and CsI photocathodes placed around the target region is used for electron identification, together with Time Of Flight (TOF/TOFINO) and an electromagnetic pre-shower detector (Pre-Shower). Particle identification is also provided using the correlation between TOF and momentum for charged pions and protons and using in addition the width of the time signal in the MDC's for charged kaons. TOF measurements in a Forward Wall scintillator hodoscope (FW) located 7 m downstream the target were used in $d + p$ reactions. It allowed

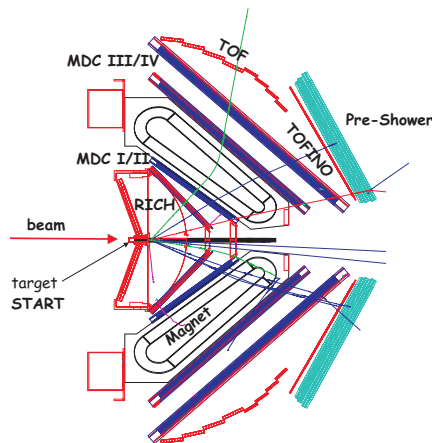


Fig. 3. HADES set-up.

indeed for the detection of forward emitted particles with the characteristics of spectator protons in order to select quasi-free $n + p$ reactions. The first level trigger selects events within a defined charged particle multiplicity range, while the second level trigger corresponds to electron candidates defined by RICH and Pre-Shower/TOF information. In the case of the $d + p$ experiment, the first level trigger also requires a coincidence with at least one particle in the FW. A 5 cm long liquid-hydrogen target (1% interaction probability) and proton and deuteron beams with intensities up to 10^7 particles/s were used.

3.5. Data analysis

e^+e^- pairs are selected using different criteria to check the track and ring qualities, as well as the identification of the electron and positron. The combinatorial background, which arises from double conversion of π^0 decay photons, conversion of the photon emitted in the π^0 Dalitz decay, or multi-pion decays, was obtained as the arithmetic mean of like-sign e^+e^+ and e^-e^- pairs and was subtracted from the measured e^+e^- sample. The correlated pairs from photon conversion are also removed, using a lower limit of 9° on the opening angle of the pair. Detection and efficiency corrections, based on GEANT simulations, are also applied, and the final spectra are normalized using the elastic (or quasi-elastic) pp scattering measured simultaneously by HADES. The overall normalization error is estimated to be 9%, the systematic error to about 20%, with a possible smooth invariant mass dependence. In the case of the $d + p$ experiment, a condition on the momentum ($1.6 \text{ GeV}/c < p_{\text{FW}} < 2.6 \text{ GeV}/c$) and on the angle ($0.3^\circ < \theta_{\text{FW}} < 6^\circ$) of the particle detected in the FW is added.

3.6. Results and comparison to models

Fig. 4 shows the dilepton mass spectra measured in the pp and quasi-free np reactions [21] compared to the simulations as described in Sec. 3.3. For both reactions, there is a good agreement between the dilepton yield measured at low invariant masses and the simulation of the π^0 Dalitz decay, which confirms the normalization and analysis procedures. In the case of the pp reaction, the region of invariant masses larger than $140 \text{ MeV}/c^2$ is also well described by the simulation of the Δ Dalitz decay. An even better agreement is obtained when the two-component quark model is used instead of the constant magnetic form factor ($G_M = 3$), which illustrates the sensitivity of these data to the electromagnetic structure of the $N-\Delta$ transition. However, the description of Δ Dalitz decay in this resonance model is too crude to extract direct information on the time-like $N-\Delta$ transition form factor. A more accurate description is expected from the OBE models, since they take into account all graphs involving intermediate Δ or nucleons. In these

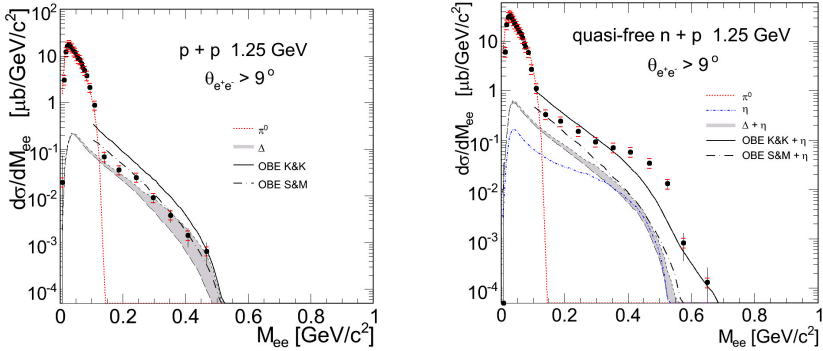


Fig. 4. Dielectron mass distribution measured in the pp (left part) and quasi-free np (right part) reactions at a beam energy of 1.25 GeV/nucleon. The dotted (red on-line) and dashed lines show the contributions of π^0 and Δ Dalitz decay, respectively, in simulations using the resonance model. The enhancement due to the N - Δ transition form factor is shown as the grey area. The dashed and full lines are the results of simulations using the OBE models [13] and [6], respectively.

models, constant form factors are used, but defined using different covariants than the usual magnetic, electric and coulomb form factors. This induces a different q^2 dependence of the differential width. This effect has again an influence at the high invariant mass end of the spectrum. The predictions of [13] (shown as dashed line) are indeed in pretty good agreement with the data. The other OBE model [6] (full line) overestimates the data.

The shape of the spectrum changes dramatically when going from $p+p$ to $n+p$ interactions. In the mass region between 0.15 and 0.35 GeV/ c^2 , the yield is about a factor 9 higher in the case of the $n+p$ reaction, while only a factor 2 is expected for the Δ Dalitz decay contribution due to the isospin factors. The resonance model simulation widely underestimates the measured dilepton yield. The η Dalitz decay contribution is rather small and the inclusion of the N - Δ transition form factor model does not help either. Nevertheless, this simulation is missing the nucleon-nucleon bremsstrahlung contribution which is expected to be in the case of the pn system much larger than in the case of pp . The comparison to the OBE exchange models is thus more relevant, but no satisfactory agreement is achieved, even with the model of [13], despite its good behaviour in the case of the pp data. To select more strictly quasi-free reactions, a smaller angular selection ($0.3^\circ < \theta_{FW} < 2^\circ$) has been applied, with no change in the shape of the invariant mass distribution. No clarification was provided either by the transverse momentum and rapidity spectra, which present very similar shapes as compared to the $p+p$ reaction.

These results are also in agreement with the DLS spectra measured in pp and pd reactions [22], with lower statistics and precision. In the case of the pd reaction, only indirect confirmation could be obtained through the comparison of the same models, while in the case of the pp reaction at 1.04 GeV and 1.27 GeV, the direct comparison was possible [23], showing a very good agreement. The interpretation of the pn dilepton spectra is still the subject of theoretical investigations, related for example, to possible ρ or ω meson off-shell production by higher-lying resonances.

These dilepton spectra measured in pp and quasi-free np experiments are used to build a reference spectrum defined by $0.5/\sigma_{\pi^0}^{NN}(d\sigma_{ee}^{pp}/dM_{ee} + d\sigma_{ee}^{pn}/M_{ee})$, where $\sigma_{\pi^0}^{NN}$ is the mean inclusive π^0 cross-section in a nucleon–nucleon collision. After subtraction of the η contributions and normalization to the π^0 multiplicities, the dilepton spectra measured in the C+C systems at 1 and 2 AGeV [21, 23, 24] are compatible with this reference spectrum [24], which hints to the fact that the excess dilepton yield measured in C+C systems is due to some additional dilepton source already present in the np system.

4. Exclusive channels in elementary reactions

Dedicated exclusive channels can be isolated, by exploiting the capability of HADES to measure charged hadrons. For example, the π^0 and η Dalitz decays could be studied in $pp \rightarrow pp e^+e^- \gamma$ reactions at 2.2 GeV, where the four charged particles are detected, the photon is reconstructed using missing four-momentum and the meson is identified by the 2 proton missing mass. The helicity angle α is then defined as the angle between the momentum vectors of the lepton in the virtual photon (γ^*) frame and of the γ^* in the decay meson rest frame. After acceptance corrections, these angular distributions are in agreement with a $1 + \cos^2 \alpha$ distribution (Fig. 5). This is a very nice

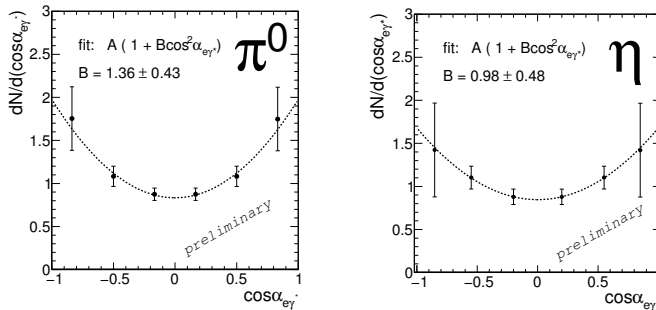


Fig. 5. Helicity angular distributions for π^0 (left panel) and η (right panel) Dalitz decays reconstructed from $pp \rightarrow pp\pi^0/\eta \rightarrow pp e^+e^- \gamma$ exclusive channels at 2.2 GeV after acceptance and efficiency corrections.

experimental check of the trend which is expected from QED, considering that, in the decay of these pseudoscalar mesons, only transverse photons can be produced. In the pp reaction at 1.25 GeV, the on-going analysis of the $pp \rightarrow ppe^+e^-$ channel is expected to bring more detailed information on the Δ Dalitz decay process and pp bremsstrahlung, like pe^+e^- invariant masses, or lepton helicity angular distribution.

Hadronic channels are also intensively studied, since they provide analysis checks, but also new physics results. The detection of both protons from $p + p$ elastic scattering allows for tracking efficiency and momentum resolution measurements. Moreover, the exclusive production of unstable particles, which present a known leptonic or Dalitz decay branching ratio, can be studied both in $pp \rightarrow pp e^+e^-X$ channels, and in purely hadronic channels, which is suited for a cross-check of the analysis efficiencies, while producing new measurements of the production cross-sections. This possibility has been exploited in the case of $pp \rightarrow pp\pi^0$ reaction at 1.25 and 2.2 GeV and $pp \rightarrow pp\eta$ reactions at 2.2 GeV. While the η case is still investigated, the exclusive π^0 production cross-section determined both in hadronic and Dalitz decay channel is found in very good agreement with existing data.

Moreover, the exclusive $pp \rightarrow pn\pi^+$ and $pp \rightarrow pp\pi^0$ measurements provide very detailed checks of the resonance model used for the analysis of the dilepton spectra [25]. As shown on Fig. 6, the yields and invariant mass

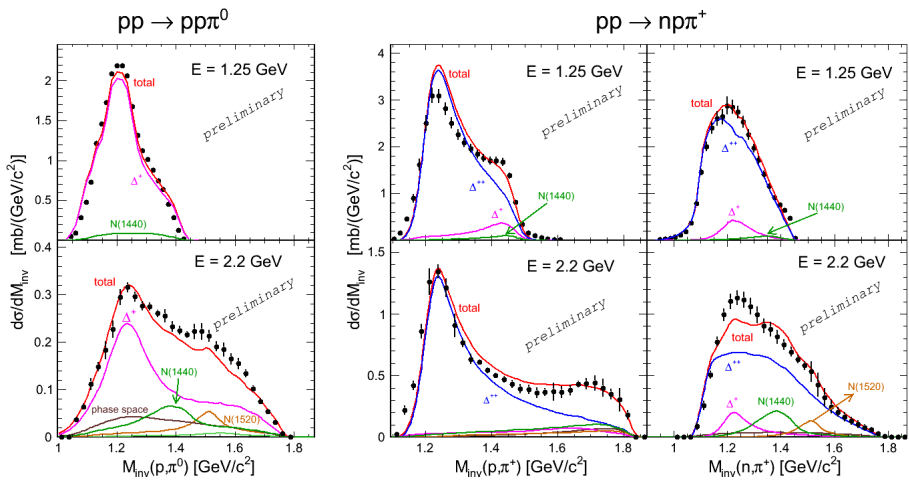


Fig. 6. πN invariant masses measured in $pp \rightarrow pp\pi^0$ and $pp \rightarrow pn\pi^+$ reactions at 1.25 and 2.2 GeV. HADES data (full dots) are compared on an absolute scale to the predictions from the resonance model, with contributions of the following resonances $\Delta^+(1232)$ (pink), $\Delta^{++}(1232)$ (blue), $N(1440)$ (green), $N(1520)$ (light brown) and $\Delta(1600)$ (light green) and an additional small phase space contribution (dark brown).

distributions are in good agreement with the simulations using an event generator based on the resonance model (see Sec. 3.3). The dominant contribution comes from the Δ resonance excitation, but $N(1440)$ and $N(1520)$ play also a significant role at 2.2 GeV. At 1.25 GeV, the relation $\sigma(pp \rightarrow pn\pi^+) = 5\sigma(pp \rightarrow pp\pi^0)$ is fulfilled, as expected from the isospin factors in the different Δ decay channels. The angular distributions are also carefully studied, since they carry detailed information on the mechanisms of Δ resonance excitation beyond the one-pion exchange.

5. Perspectives from pion induced reactions

The dilepton spectroscopy in π induced experiments on nuclei is proposed in order to study medium effects on ρ and ω mesons, with the advantages, with respect to heavy-ion induced reactions, of higher expected effects on ω meson and reduced combinatorial background. This would also complement the on-going studies of ρ/ω production at normal nuclear density in the $p+\text{Nb}$ system. Due to the well-known interaction and the possibility of exclusive channel measurements, the reactions on nucleon constitute a unique tool to study ω and ρ production, with a special interest of subthreshold production via the coupling to baryonic resonances. In particular, in [26], a spectacular destructive ρ/ω interference is predicted below the ω threshold. As these couplings are related to the electromagnetic structure of the resonances, these measurements present a fundamental interest.

Strangeness production measurements with pion beam induced reactions is also possible. This includes $\Lambda(1405)$ production in π^-p reactions at an incident momentum around 1.7 GeV/ c , in medium modifications and K^- absorption in π^-p and π^-A reactions at 1.7 GeV/ c , and K_S^0 production in $\pi^- + p$, $\pi^- + \text{C}$ and $\pi^- + \text{Pb}$ at lower energies.

From the technical point of view, some developments are still needed to check the feasibility of these experiments. An intensity of 10^6 particles/s is needed, which is in principle accessible and fast and thin position sensitive beam detectors are under study to fully reconstruct the trajectory and momentum of incident pions.

6. Conclusion

Recent HADES results have been discussed, with emphasis on the elementary reactions, which allow to build a reference for the heavy-ion measurements, and help to clarify the controversial problem of contribution of Δ Dalitz decay and Bremsstrahlung processes. The interpretation of the inclusive pn spectra remains however challenging. More selective information on the Δ Dalitz decay and bremsstrahlung processes is expected from the analysis of the exclusive $pp \rightarrow ppe^+e^-$ reaction.

HADES is currently being upgraded in order to handle more efficiently the higher multiplicities related to the heavier systems, like Ag+Ag and Au+Au. Pion beam experiments also offer interesting perspectives to clarify the role of higher lying resonances. Although the specificity of HADES is the dilepton spectroscopy with a large angular acceptance and good precision, the variety of all these measurements demonstrates the power of HADES as a multipurpose detector.

REFERENCES

- [1] [HADES Collaboration] G. Agakichiev *et al.*, *Phys. Rev. Lett.* **98**, 052302 (2007).
- [2] [HADES Collaboration] G. Agakichiev *et al.*, *Phys. Lett.* **B663**, 43 (2008).
- [3] [DLS Collaboration] R. Porter *et al.*, *Phys. Rev. Lett.* **79**, 1229 (1997).
- [4] E. Bratkovskaya, W. Cassing, *Nucl. Phys.* **A807**, 214 (2008).
- [5] M. Thomere, C. Hartnack, G. Wolf, J. Aichelin, *Phys. Rev.* **C75**, 64902 (2007); E. Santini *et al.*, *Phys. Rev.* **C78**, 34910 (2008); K. Schmidt *et al.*, *Phys. Rev.* **C79**, 64908 (2009); H.W. Barz *et al.*, [arXiv:0910.1541](https://arxiv.org/abs/0910.1541) [nucl-th].
- [6] L.P. Kaptari, B. Kämpfer, *Nucl. Phys.* **A764**, 338 (2006).
- [7] R. Shyam, U. Mosel, *Phys. Rev.* **C67**, 065202 (2003).
- [8] [HADES Collaboration] F. Krizek *et al.*, [arXiv:0907.3690](https://arxiv.org/abs/0907.3690) [nucl-ex].
- [9] C. Gale, J. Kapusta, *Phys. Rev.* **C35**, 2107 (1987).
- [10] M.I. Krivoruchenko, A. Faessler, *Phys. Rev.* **D65**, 017502 (2002).
- [11] M. Zetenyi, G. Wolf, [arXiv:0202047](https://arxiv.org/abs/0202047) [nucl-th].
- [12] G. Wolf *et al.*, *Nucl. Phys.* **A517**, 615 (1990).
- [13] R. Shyam, U. Mosel, *Phys. Rev.* **C79**, 035203 (2009).
- [14] Q. Wan, F. Iachello, *Int. J. Mod. Phys.* **A20**, 1846 (2005); Q. Wan, Ph.D. thesis, Yale University, New Haven, USA, 2007.
- [15] I. Fröhlich *et al.*, *POS (ACAT)*, 076 (2007) [[arXiv:0708.2382](https://arxiv.org/abs/0708.2382)].
- [16] F. Dörhmann, [arXiv:0909.5373](https://arxiv.org/abs/0909.5373) [nucl-ex].
- [17] S. Teis *et al.*, *Z. Phys.* **A356**, 421 (1997).
- [18] J. Bistricky, F. Lehar, *J. Phys.* **48**, 1901 (1981).
- [19] P. Moskal *et al.*, *Phys. Rev.* **C79**, 015208 (2009).
- [20] [HADES Collaboration] G. Agakichiev *et al.*, *Eur. Phys. J.* **A41**, 243 (2009).
- [21] [HADES Collaboration] G. Agakishiev *et al.*, [arXiv:0910.5875](https://arxiv.org/abs/0910.5875) [nucl-ex], submitted to *Phys. Rev. Lett.*
- [22] W. Wilson, *Phys. Rev.* **C57**, 1865 (1998).
- [23] T. Galatyuk, Ph.D. thesis, Frankfurt University, Germany, 2009.
- [24] J. Stroth, talk at the XXXI Mazurian Lakes Conference on Physics, Piaski, Poland, August 30–September 6, 2009, not included in the Proceedings.
- [25] M. Wisniewski, Ph.D. thesis, Jagellonian University, Poland, 2009; [HADES Collaboration] T. Liu *et al.*, [arXiv:0909.3399](https://arxiv.org/abs/0909.3399) [nucl-ex].
- [26] A.I. Titov, B. Kämpfer, *Eur. Phys. J.* **A12**, 217 (2001); M. Lutz, B. Friman, M. Soyeur, *Nucl. Phys.* **A713**, 97 (2003).